

Supporting Information

Structure and Phase Changes of Alumina Produced by Flame Hydrolysis

Jamal Nasir¹, Franz Schmidt², Frank Menzel², Jörn Schmedt auf der Günne^{1*}

*1 University of Siegen, Faculty IV: School of Science and Technology, Department of Chemistry and Biology,
Inorganic materials chemistry and Center of Micro- and Nanochemistry and Engineering (Cμ), Adolf-
Reichwein-Straße 2, D-57076 Siegen, Germany*

2 Evonik, Operations GmbH, Rodenbacher Chaussee 4, D-63457 Hanau, Germany

*Email: gunnej@chemie.uni-siegen.de

Figure S1: Rietveld refinement as γ -alumina (S200 and S180)

Table S1: Parameters for Rietveld Refinement for the Sample S220

Figure S2: Spectral Simulations of ^{27}Al MAS NMR Spectra

Table S2: Spectral Parameters Determined by Simulations Using the DMfit Software:

Figure S3: ^{27}Al MQMAS Spectra of Fumed Alumina for the S220 to S45 Samples

Figure S4: Projections of ^{27}Al MQMAS Spectra of Fumed Alumina for the S220–45 Samples

Figure S5: Aging Effect on the Local Structure of high BET Fumed Alumina

Figure S6: TEM Images of Fumed Alumina for the S220 to S30 Samples

Figure S7: Histograms for Particles Sizes for the S220 to S30 Samples

Figure S8: High-resolution TEM images of S65.

Rietveld Refinement of the X-ray Patterns as γ -Alumina for the S200 and S180 Samples

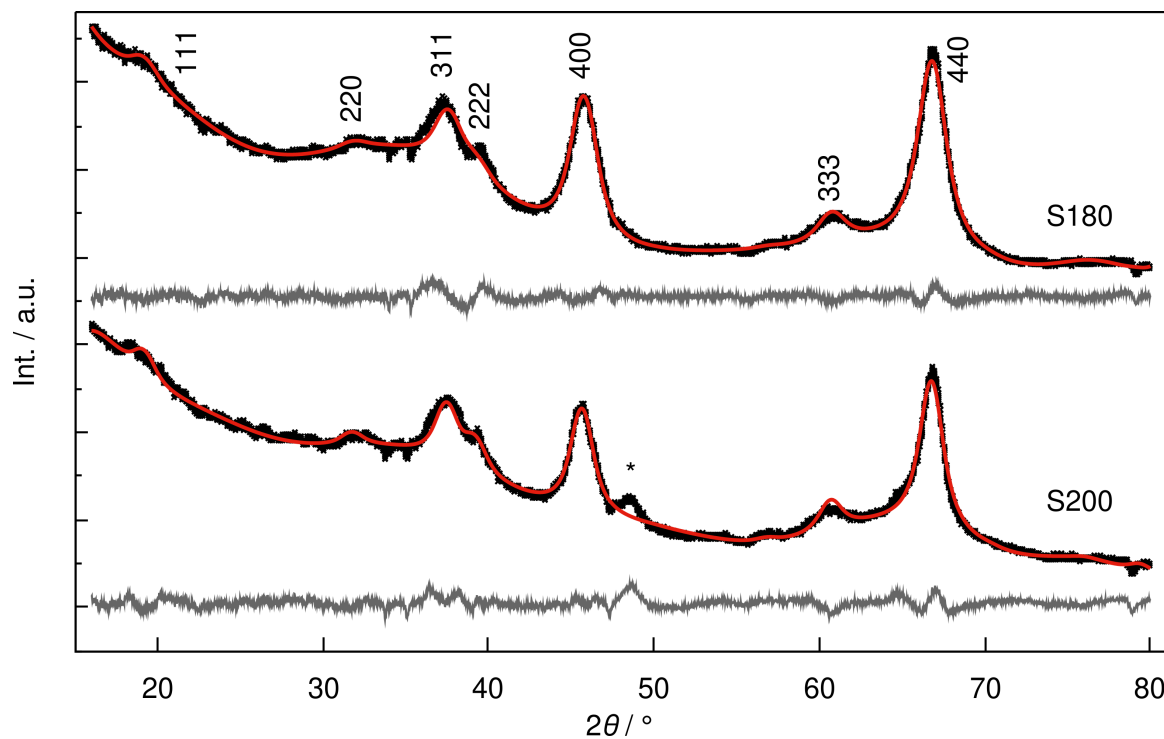


Figure S1: Rietveld refinement of the X-ray diffraction pattern for the S200 and S180 samples using Smrcok et al. spinel model for γ -alumina with a significant amount of non-spinel occupation. The black points represent the experimental data, the red solid line the calculated diffractogram with a residual profile factor R_{wp} respectively of 3.6% and 3.2%, and the grey line the difference plot. The peak marked with asterisk * is non-existent in γ -alumina.

Parameters for Rietveld refinement of γ -alumina (S220)

Table S1: Exemplary Rietveld refinement input file (used in Topas academic package^[1]) with the refined parameters for the S220 sample powder diffraction (Figure 2) recorded on Guinier camera.

```
r_wp 3.02719
r_exp 2.61441499
r_p 2.25241953
gof 1.15788427

iters 100000
chi2_convergence_criteria 0.001
do_errors

xdd BET220.xy

x_calculation_step = Yobs_dx_at(Xo); convolution_step 4
bkg @ 1376.83569`_1.42975713
-1071.80372`_1.87856674
189.442678`_1.8611632
-4.44479503`_1.74830992
-136.84087`_1.68499227
-49.7694861`_1.50821558
134.965508`_1.66444081
12.9518863`_1.93736098
-75.5144272`_1.49218123
-12.6398723`_1.49710774
15.7383351`_1.43657743
-13.0475097`_1.29415789
24.2915403`_1.12030175
16.4935932`_1.31027513

LP_Factor(!th2_monochromator, 27.28)          'd8 Ge(111) monochromator Vantec Cu Ka1
CuKa1(0.0001)

Specimen_Displacement(height, 0.592872541`_42.5013868)
Specimen_Tilt(@, 1.10207389`_0.0500654427)
```

```
Divergence( 0.823576214_0.00574586197 )
Simple_Axial_Model(!axial, 2.15331558_0.00498608309)
Tube_Tails(, 0.00487350562,, -0.0388314018,, 0.00329872058_LIMIT_MIN_1e-05,,,
0.0620669557)
```

Rp 220

Rs 57.3

```
'th2_offset
```

```
prm a1 -1.57056476`_39.9589523
prm a2 1.38586295`_4.13264432
prm a3 0.644076644`_85.1791326
```

```
th2_offset = a1 Th^2 + a2 Th^1 + a3;
```

```
start_X 16
```

```
finish_X 80
```

```
Out_Yobs_Ycalc_and_Difference("S220_Yobs_Ycalc_and_Diff.txt")
Out_X_Yobs("S220_Out_X_Yobs .txt")
```

```
str
```

```
phase_name gamma-Al2O3
space_group "F d -3 m Z"
Cubic (@ 7.933079`_0.263268)
volume 499.258`_49.710
```

```
site Al1 x = 0.125; y = 0.125; z = 0.125; occ Al+3 @ 0.42634`_0.00754 beq 0.489532378
site Al2 x = 0.5; y = 0.5; z = 0.5; occ Al+3 @ 0.60394`_0.00511 beq 0.726402884
site O1 x = 0.25673; y = 0.25673; z = 0.25673; occ O-2 1 beq 0.876420871
site Al3 x = 0.0; y = 0.0; z = 0.0; occ Al+3 @ 0.24762`_0.00435 beq 0.710611517
site Al4 x = -0.123; y = 0.125; z = 0.125; occ Al+3 @ 0.08999`_0.00264 beq 0.473741011
```

```
LVol_FWHM_CS_G_L(1, 5.19609424`_0.422947564, 0.89, 7.26466565`_0.581104289, , ,
cslc, 8.16254567`_0.652926168)
```

```
e0_from_Strain( 2.18048578e-07`_0.000379272174, , , slc, 0.0001`_0.173939301) 'eo single
strain value from Gaussian / Lorentzian
```

```
scale @ 0.00120704504`_1.678e-05
r_bragg 0.205480314
Phase_Density_g_on_cm3( 3.61930318`_0.360609447)
```

Spectral Simulations of ^{27}Al MAS NMR Spectra

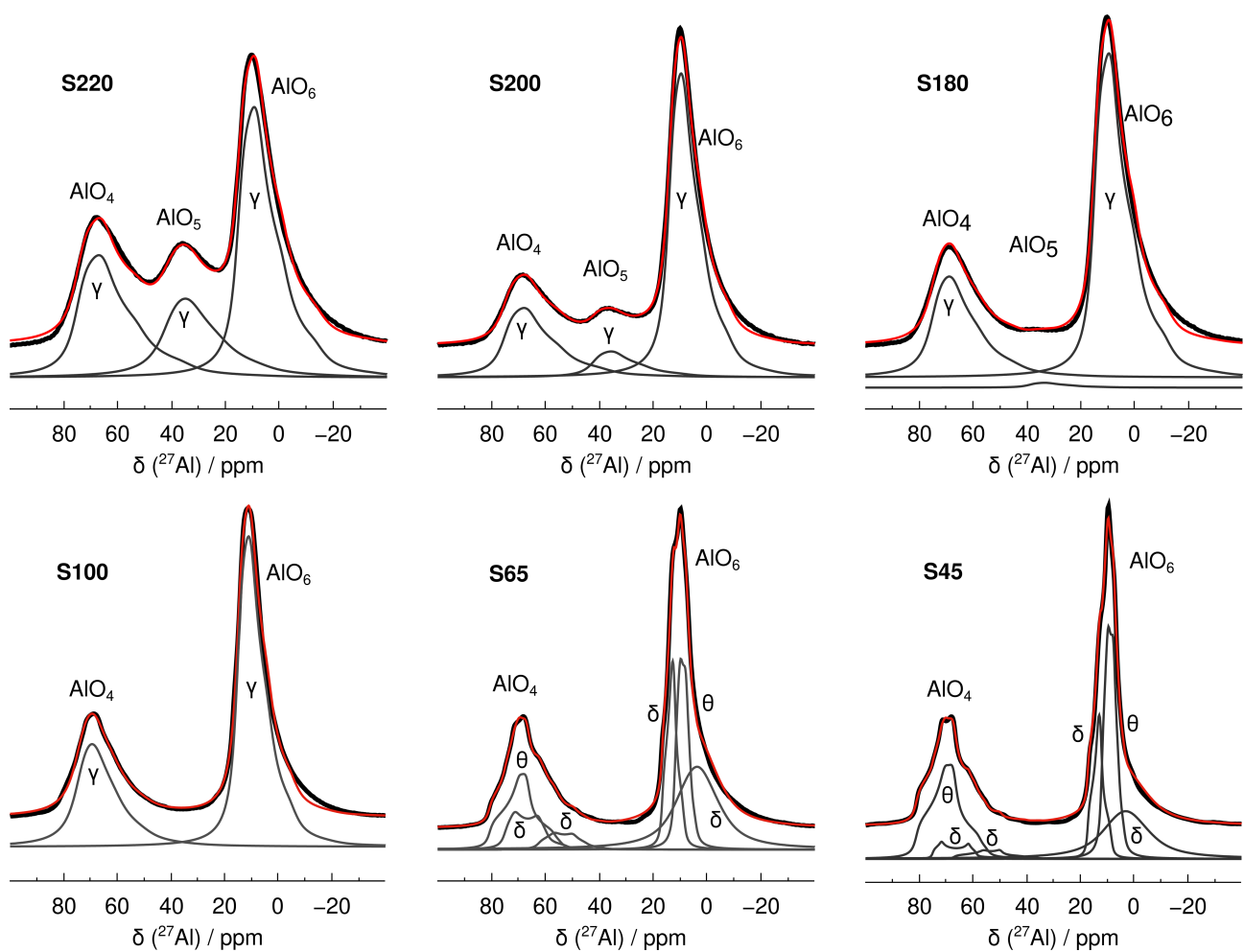


Figure S2: ^{27}Al MAS NMR spectra simulated using Czjzek model for S220 to S100 samples, using Q mas 1/2 model for the S65–45 samples as implemented in DMfit software.^[1] The experimental data are shown in black, the total simulated spectra in red, and the individual decomposed spectra in grey.

Spectral Parameters Determined by Simulations Using DMfit Software

Table S2: ^{27}Al MAS NMR parameters for the AlO_4 , AlO_5 and AlO_6 sites in fumed alumina materials obtained by using Dmfit package and the corresponding literature values.

BET m^2/g	Main phase	Site	δ_{iso} / ppm	C_Q MHz	η	Model used	Relative intensities	Comment
γ -alumina	γ -alumina	AlO_4	77.5 ± 0.2	3.5 ± 0.1		Czjzek	10%	^[2] DNP NMR
		AlO_5	37.2 ± 0.2	4.5 ± 0.1			13%	
		AlO_6	14.0 ± 0.2	4.3 ± 0.1			78%	
δ -alumina	δ -alumina	AlO_4	73.2	4.6	0.6		19.6%	^[3] Al isopropoxide precursor; sol- gel
		AlO_4	68.3	6.6	0.4		20.7%	
		AlO_6	16.3	4.8	0.0		25.8%	
		AlO_6	14.5	4.3	0.6		33.9%	
θ -alumina	θ -alumina	AlO_4	80 (1)	6.4 (0.1)	0.65(0.02)		47.8%	^[4] Al tributoxide precursor; sol- gel
		AlO_6	10.5 (1)	3.5 (0.3)	0(0.1)		52.2%	
S220	γ -alumina	AlO_4	75	6.6		Czjzek	30.1%	This study
		AlO_5	42	6.2			21.5%	
		AlO_6	15.3	5.6			48.4%	
S200	γ -alumina	AlO_4	75.2	6.3		Czjzek	24.5%	This study
		AlO_5	42.2	6			8.6%	
		AlO_6	14	4.9			66.9%	
S180	γ -alumina	AlO_4	75	5.8		Czjzek	28.8%	This study
		AlO_5	39	5.5			1.2%	
		AlO_6	15	5.4			70%	
S130	γ -alumina	AlO_4	74.4	5.4		Czjzek	31%	This study
		AlO_6	15	5.1			69%	
S100		AlO_4	74.4	5.1		Czjzek	33%	This study
		AlO_6	15.0	4.7			66.7%	
S65	θ -alumina	AlO_4	80.9	6.3	0.8	Q mas	17.9%	This study

		AlO ₆	12.3	3.6	0.4	1/2	19%	
	δ -alumina	AlO ₄	77	6.3	0.3		9.5%	
		AlO ₄	64	6.3	0.4		4.5%	
		AlO ₆	16.6	3.5	0.8		16.2%	
		AlO ₆	11.1	5	0.7		32.8%	
		AlO ₄	81.3	6.3	0.8	Q mas 1/2	27%	This study
	θ -alumina	AlO ₆	12.4	3.7	0.5		27.3%	
		AlO ₄	77.4	6.6	0.2		4.1%	
		AlO ₄	67.6	7.1	0.6		3%	
		AlO ₆	17.3	3.6	0.8		14%	
		AlO ₆	10.8	5	0.9		24.7%	
	θ -alumina	AlO ₄	80.4	6.1	0.9	Q mas 1/2	15.6%	This study
		AlO ₆	12.7	3.9	0.5		18.3%	
		AlO ₄	76.6	6.4	0.2		8%	
		AlO ₄	73.3	8.3	0.7		9%	
		AlO ₆	16.4	3.3	1		24.1%	
	δ -alumina	AlO ₆	10.2	5.2	0.7		25%	

^{27}Al MQMAS Spectra of Fumed Alumina for the S220–45 Samples

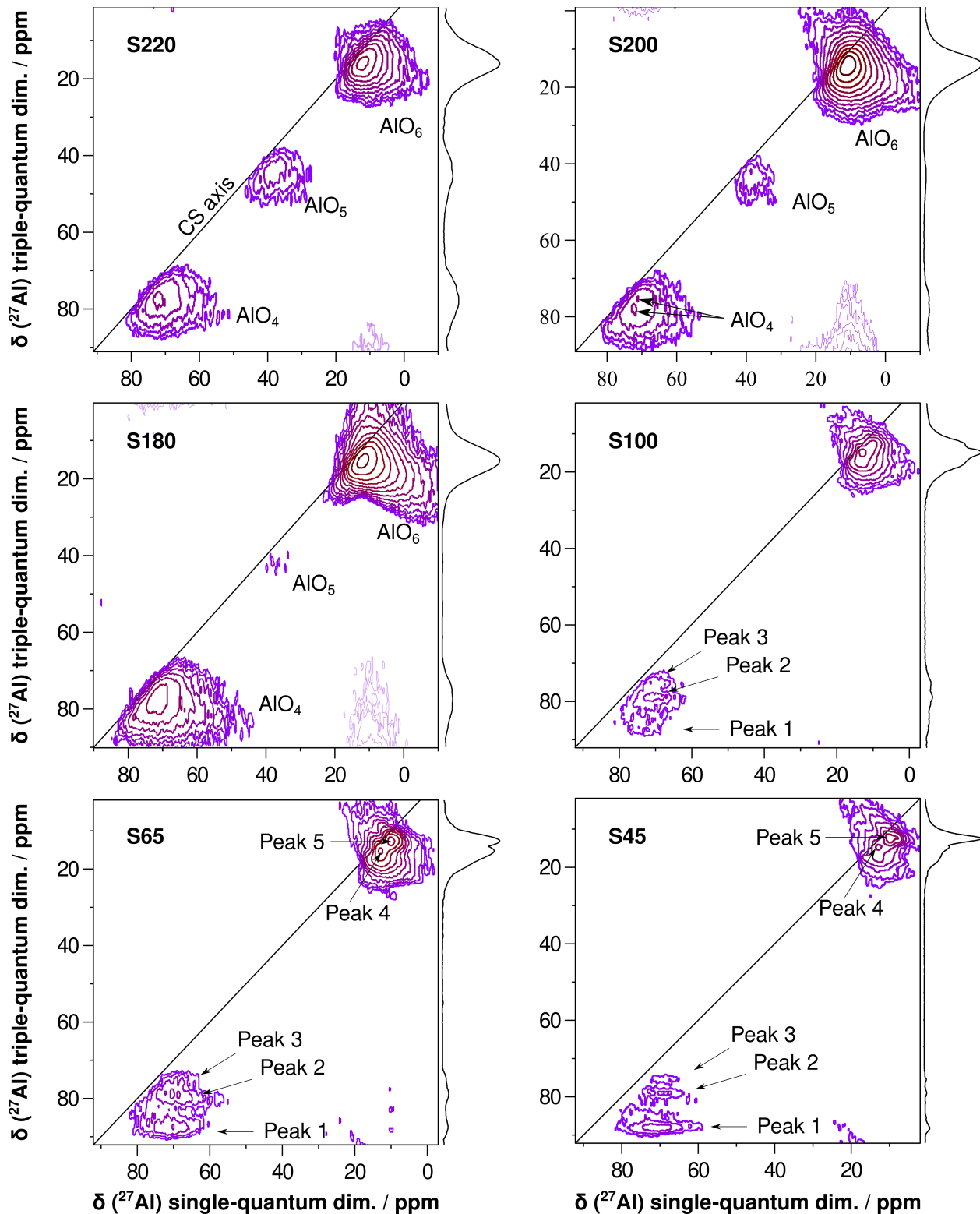


Figure S3: Sheared ^{27}Al triple-quantum MQMAS NMR spectra of fumed alumina for the S220 to S45 samples measured at 20 kHz MAS frequency. The sum projection of the isotropic spectra are shown on the right of each 2D spectrum.

Projections of ^{27}Al MQMAS Spectra of Fumed Alumina for the S220–45 Samples

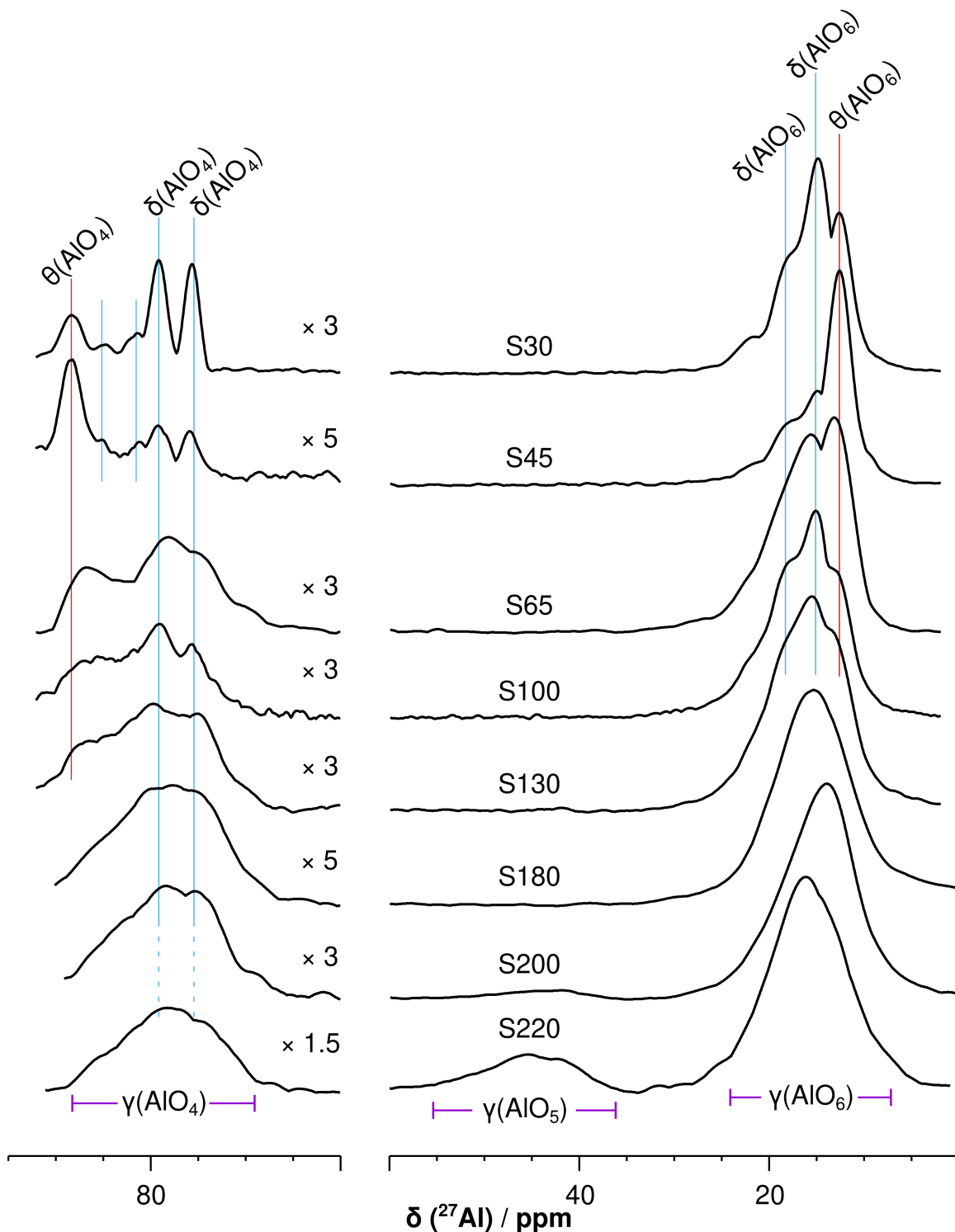


Figure S4: Sum projections of ^{27}Al triple-quantum MQMAS spectra of fumed alumina samples with S220–30 measured at 20 kHz MAS frequency. In the shearing execution, not all the 2D spectra are shifted by the same value.

Aging Effect on the Local Structure of High BET Fumed Alumina

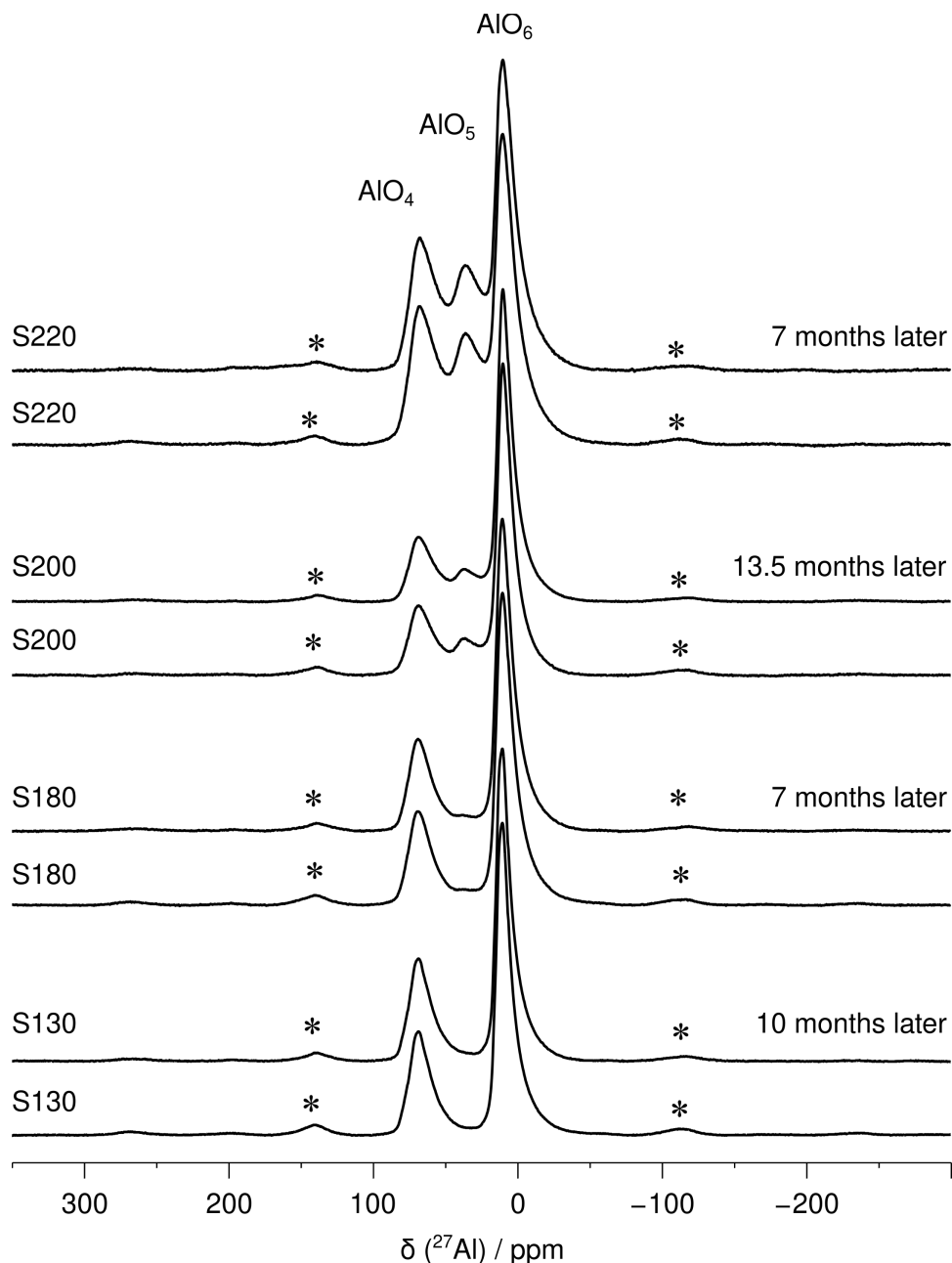


Figure S5: ^{27}Al MAS NMR spectra intended to reveal an aging effect on the samples S220 to S130 measured at 20 kHz MAS frequency a second time after various periods of time. As is obvious, there is no noticeable change in the shape or intensities of the spectra.

TEM Images of Fumed Alumina for the S220 to S30 Samples

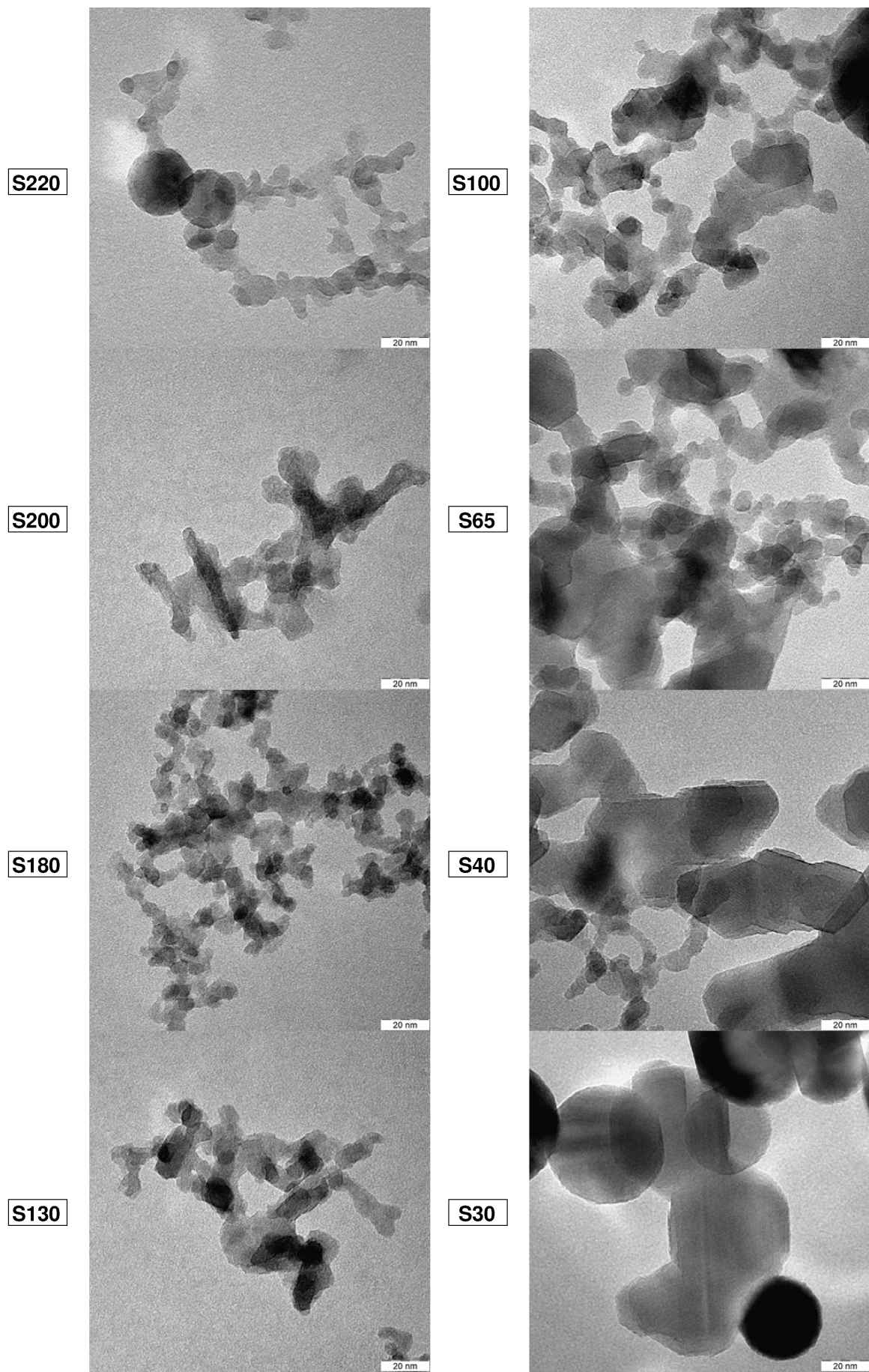


Figure S6: TEM images of fumed alumina samples S220 to S30 samples.

Histograms for Particles Sizes for the S220 to S30 Samples

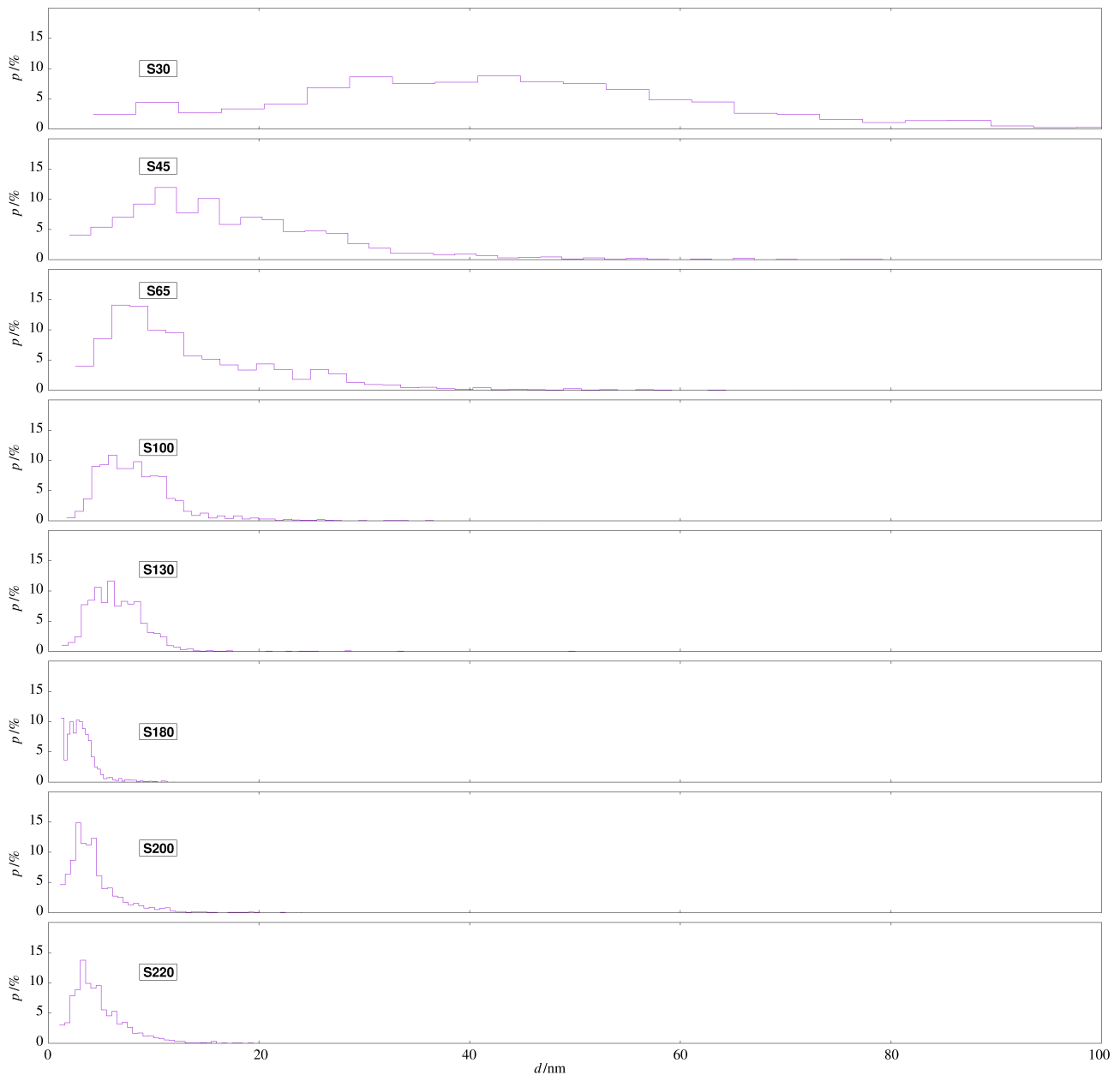


Figure S7: Particle size distribution of the fumed alumina samples S220 to S30 obtained by analysis of TEM micrographs of about 2000 particles each. For agglomerates the primary particles were counted.

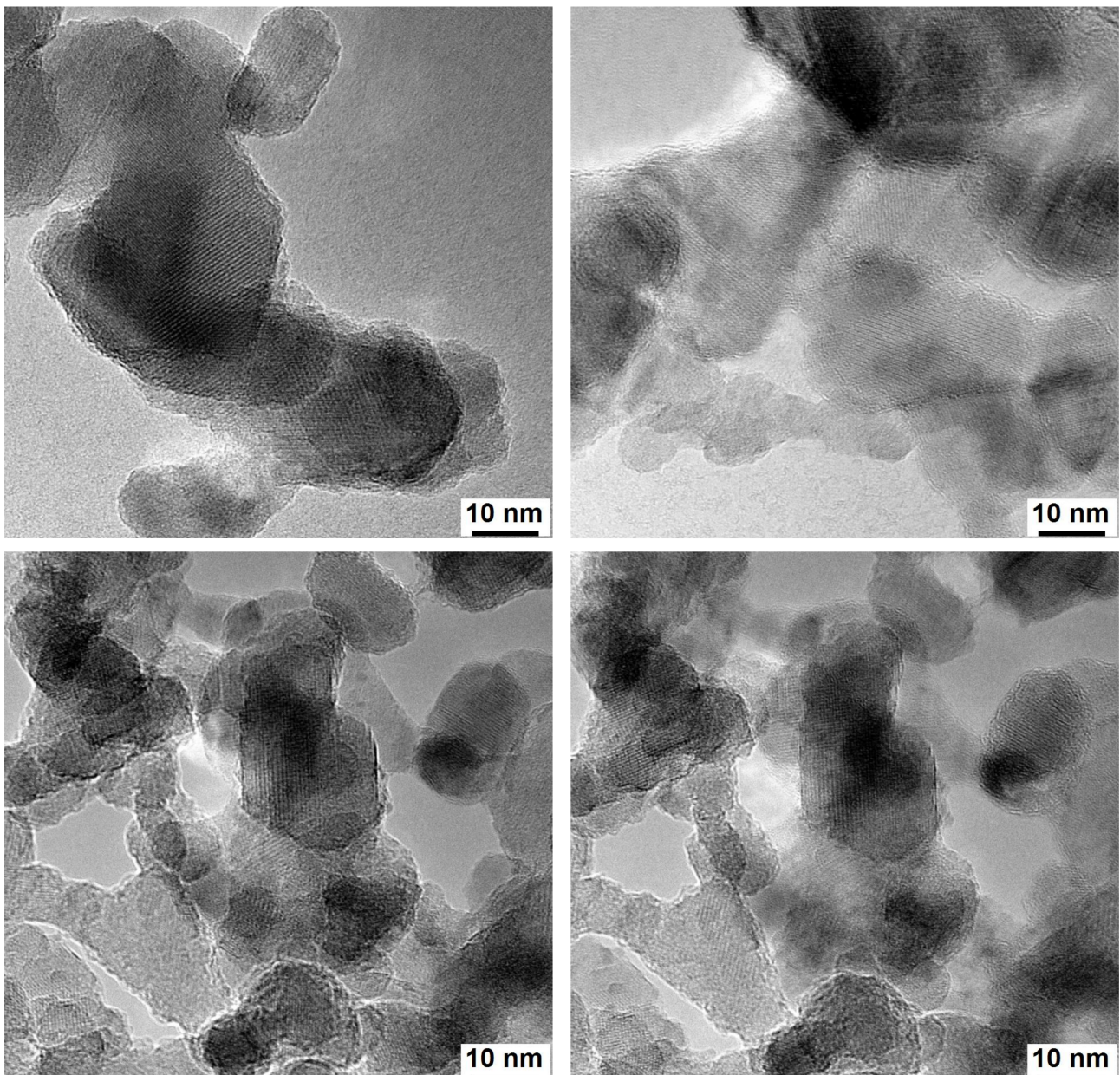


Figure S8: High-resolution TEM pictures of fumed alumina S65. The picture sure primary particles of different sizes which are the result of nucleation (small monocrystalline particles), collision and coalescence (bigger monocrystalline particles) and agglomeration and aggregation (bigger polycrystalline particles).

References

- [1] A.A. Coelho, J. Appl. Cryst. 51 (2018) 210–218.
- [2] M. Mais, S. Paul, N.S. Barrow, J.J. Titman, Johnson Matthey Technol. Rev. 62 (2018) 271–278.
- [3] S. Xu, N.R. Jaegers, W. Hu, J.H. Kwak, X. Bao, J. Sun, Y. Wang, J.Z. Hu, ACS Omega 6 (2021) 4090–4099.
- [4] L.A. O'Dell, S.L.P. Savin, A.V. Chadwick, M.E. Smith, Solid State Nucl. Magn. Reson. 31 (2007) 169–173.